Jurnal Teknologi

Full Paper

DELAMINATION DETECTION IN THIN-WALLED COMPOSITE STRUCTURES USING ACOUSTIC PITCH-CATCH TECHNIQUE WITH FIBER BRAGG GRATING SENSORS

Z. M. Hafizi[a]*, I. N. Ibrahim[a], E. Vorathin[b]

[a]Advanced Structural Integrity and Vibration Research (ASIVR), Faculty of Mechanical & Automotive Engineering Technology, Universiti Malaysia Pahang (UMP), 26600 Pekan, Pahang, Malaysia
[b]Department of Mechanical Engineering, Universiti Teknologi PETRONAS, 32610 Bandar Seri Iskandar, Perak, Malaysia

Article history
Received
30 May 2022
Received in revised form
27 December 2022
Accepted
1 February 2023
Published Online
19 April 2023

*Corresponding author
hafizi@ump.edu.my

Graphical abstract

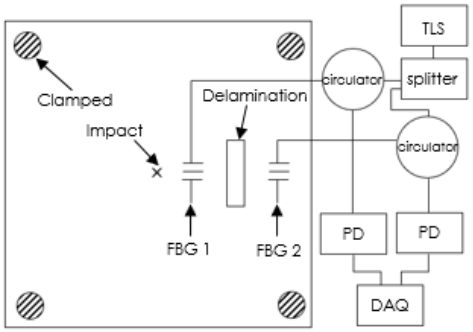

Abstract

Structural health monitoring (SHM) of a composite structure is essential in maintaining the integrity of the structure. Over the years, various studies have reported on the use of conventional electrical sensors in analysing acoustic wave propagation for delamination detection. However, electrical sensors are associated with drawbacks such as high signal attenuation, are prone to electromagnetic interference (EMI) and are not suitable for harsh environments. Therefore, this paper reported on the use of fiber Bragg grating (FBG) sensors for delamination detection. Two composite structures with delamination sizes of 10 cm × 2 cm and 10 cm × 6 cm were fabricated. Two FBGs were bonded before and after the delamination. In addition, three trials of impacts were induced at the centre of the structure. Multiple signal parameters were obtained and analysed, which were the time delay, amplitude difference and velocity difference. The experimental results revealed that the time delay, amplitude and velocity analysis varied for both the delamination sizes with an average percentage of 42.36%, 97.09% and 42.39%, respectively. Therefore, it was confirmed that the increase in delamination size resulted in a longer time delay, higher signal amplitude attenuation and slower wave propagation.

Keywords: Fiber Bragg grating (FBG), thin-walled composite structures, acoustic waves, delamination, structural health monitoring (SHM)

Abstrak

Pemantauan kesihatan struktur (SHM) bagi struktur komposit adalah penting dalam mengekalkan integriti struktur. Selama bertahun-tahun, pelbagai kajian telah melaporkan penggunaan penderia elektrik konvensional dalam menganalisis perambatan gelombang akustik untuk pengesanan delaminasi. Walau bagaimanapun, penderia elektrik dikaitkan dengan kelemahan seperti pengecilan isyarat yang tinggi, terdedah kepada gangguan elektromagnet (EMI) dan tidak sesuai untuk persekitaran yang keras. Oleh itu, kertas kerja ini melaporkan penggunaan penderia gentian Bragg grating (FBG) untuk pengesanan delaminasi. Dua struktur komposit dengan saiz delaminasi 10 cm × 2 cm dan 10 cm × 6 cm telah dibuat. Dua FBG telah diikat sebelum dan selepas delaminasi. Di samping itu, tiga ujian impak telah diinduksi di tengah-tengah struktur. Parameter isyarat berbilang telah diambil dan dianalisis, iaitu kelewatan masa, perbezaan amplitud dan perbezaan halaju. Keputusan eksperimen menunjukkan bahawa kelewatan masa, amplitud dan analisis

halaju berbeza-beza untuk kedua-dua saiz penyimpangan dengan purata peratusan masing-masing 42.36%, 97.09% dan 42.39%. Oleh itu, telah disahkan bahawa peningkatan dalam saiz delaminasi mengakibatkan kelewatan masa yang lebih lama, pengecilan amplitud isyarat yang lebih tinggi dan perambatan gelombang yang lebih perlahan.

Kata kunci: Penderia gentian parutan Bragg (FBG), struktur komposit nipis, gelombang akustik, delaminasi, pemantauan kesihatan struktur (SHM)

1.0 INTRODUCTION

Composite structure has been widely used in multiple engineering applications due to advantages such as lightweight, high strength, corrosion resistance and many more [1-3]. During long services, composite structures are often prone to barely visible impact damage (BVID) such as delamination [4-6]. Therefore, structural health monitoring (SHM) of the composite structure is crucial preventing the propagation of delamination and weakening structural integrity. Delamination detection via acoustic wave propagation is the most widely reported. An acoustic wave is a mechanical wave resulting from a vibration generated from a source [7]. Longitudinal waves, shear waves, Rayleigh waves and Lamb waves are examples of acoustic waves [7]. Lamb waves are commonly generated in a thin-walled structure that provides the through-the-thickness assessment for internal defect detection [8]. Moreover, carbon fiber-reinforced plastic (CFRP) laminates are widely used as structural materials due to their high specific strength and stiffness. The failure process of CFRP laminates under static or dynamic loadings is known to involve unique microscopic damages, such as matrix cracks and delamination. The delamination particularly can cause stiffness reduction and often leads to catastrophic failure. For engineering applications, delamination detection is very important to evaluate the reliability of CFRP laminates[9].

Investigation into FBG sensing for delamination detection remains a relatively small field of activity. Perhaps this occurred due to the mixed uneven strain fields that result from growing delamination cracks that cause the FBG's reflected spectral response to have multiple peaks, with no simple means of interpretation. To overcome this problem, a few researchers used short gauge length sensors or bond the sensors to the surface of the specimen [10],[11]. Other researchers intentionally placed FBG sensors in the non-uniform strain field [12],[9],[13],[14]. However, the FBG reflection spectrum alone could not capture the location and direction of the delamination growth due to its mixed form caused by the nonhomogeneous strain field near the delamination. Nonetheless, chirped FBG sensors have also been used to improve the sensor's ability to detect the location of the microcracks and delamination direction [13].

Over the years, acoustic emission (AE) sensors and piezoelectric transducers (PZT) are the conventionally reported sensors in capturing acoustic waves. Wang *et al*. [15] reported on the use of piezoelectric composite material as structural and sensing elements in analysing the propagation and interaction of guided waves with damage. The results showed that piezoelectric composite material possessed great potential in performing SHM. Zhao *et al*. [16] reported on utilising multiple PZTs in monitoring the delamination of composite double cantilever beams. The signals captured by the PZTs were post-processed using the Hilbert transform, Fourier transforms, and wavelet transform. The results showed that the delamination length affects the time of arrival and higher frequency modes. Hervin *et al*. [17] utilised PZT to investigate the scattering of Lamb wave mode on a delaminated composite structure. The results showed that the delamination depth significantly influenced the amplitude of the waves. Aggelis *et al*. [18] mounted eight AE sensors on a hybrid cement reinforced with a composite hollow beam to monitor the matrix cracking and delamination. The results showed that matrix cracking resulted in higher frequency values whereas delamination resulted in lower frequency values. Li *et al*. [19] utilised two AE sensors to investigate the influence of delamination length in composite cantilever beam on rise angle and strain energy release rate of the waveforms. The results showed that both parameters can be effectively used in delamination detection. Saeedifar *et al*. [20] utilised AE sensors to analyse the BVID in laminated composite structures. Here, two composite specimens were subjected to indentation loading. The waveforms captured by the AE sensors were analysed by using b-value and sentry function methods. The results showed that AE was a good sensor to determine BVID in laminated composites.

Yet, all the above-mentioned studies employed conventional electrical sensors. Electrical sensors are often associated with various disadvantages such as high signal attenuation, prone to electromagnetic interference (EMI) and are not suitable for the harsh environment [21, 22]. These drawbacks can be overcome by using of fiber optic sensors. Fiber Bragg grating (FBG) sensors are the most reported fiber optic sensors that have the advantages such as small-sized, immunity to EMI and suitable for harsh environment [23-27]. Bucaro *et al*. introduced a compact

directional acoustic sensor [28] based on a previous work [29], the microphone, that was based on a past reported fiber-lever probe [30]. Besides, the sensor was combined with a two-fiber optical probe, an optical source, a photo-detector, and a slender cylindrical cantilever to the optical reflector. At the same time, one fiber was used to describe the cantilever, the other fibers collected the reflected optical signal and was responsible for the directionality sensitivity. Furthermore, directionality is executed by the fact that the power in the collection fiber varies proportionally to the cosine of the angle between the axis of the two fibers and the cantilever tip displacement direction which, in turn, is in the same direction as the acoustic wave. The most responsive fiber-optic acoustic sensors reported up to now are based on FP cavities, and recent works suggested that this could be further enhanced by using diaphragms of different materials with increased stiffness and a lower thickness-to-diameter ratio. In addition, FBGs are most suitable for multiplexing, since wavelength multiplexing is easier to implement than time-domain multiplexing. Although this technology typically exhibits lower sensitivities, recent developments have been overcoming this problem according to [31]. Besides, fiber-optic Michelson interferometers are also used in the context of acoustic detection, since it was demonstrated for the first time in 1980 [32], [33]. The Michelson configuration consists of an optical fiber coupler whereby two output arms are used as reference and sensor routes. At the end of each arm, there is a reflecting structure to send the two signals back to the detector. All these papers reported on the use of FBG sensors in capturing acoustic wave propagation for delamination detection in thin-walled composite structures.

Additionally, in this present work multiple signal parameter analysis was enforced to improve the level of confidence in the detection of delamination growth. For any existing structures, FBG sensors can be attached to their surfaces; and for new structures, FBG sensors can be embedded into them during fabricating stage without affecting the integrity. As the result, the output signal from this SHM system could show an early warning of the structural integrity to prevent serious losses and avoiding catastrophic failures.

2.0 METHODOLOGY

2.1 Fabrication of specimens

Two delaminated composite structures were fabricated with the hand lay-up method. The composite structure consisted of four layers of fiberglass. The fiberglasses which were arranged as chopped strand mat (CSM) 450 with 0° orientation, woven roving 300 with 90° orientation, woven roving 300 with 45° orientation and CSM 450g with -45°. Reversal P-9509 NW was used as the resin and Butanox M-60 methyl ethyl ketone peroxide (MEKP) was used as the curing agent. The composite structure had a dimension of 90 cm length × 90 cm width × 0.3 cm thickness, as shown in Figure 1(a).

Delamination was formed 15 cm away from the centre of the structure. The delamination was fabricated by inserting CSM 450 and tissue mat into the middle layer of the fiberglass. The first composite structure had a delamination size of L = 10 cm and H = 2 cm. Meanwhile, the second composite structure had a delamination size of L = 10 cm and H = 6 cm. Each composite structure was surface bonded with two FBG sensors as shown in Figure 1(b). FBG 1 was bonded 8 cm away from the centre of the structure. Whereas, FBG 2 was bonded 23 cm away from the centre of the structure. Ultraviolet (UV) adhesive glue was utilised for the bonding process.

The FBG sensor consisted of a short segment of Bragg grating that reflected the Bragg wavelength (λ_B) which is expressed as [1]:

$$\lambda_B = 2\eta_e \Lambda \quad (1)$$

Where, η_e is the effective refractive index and Λ is the grating period. At the temperature of 26.8 °C, the Bragg wavelength for FBG 1 and FBG 2 of the first composite structure was recorded at 1549.9869 nm and 1549.9946 nm respectively. For the second composite structure, wavelength of FBG 1 and FBG 2 was recorded at 1549.9640 nm and 1549.8739 nm respectively. All the wavelength measurements were recorded by using the optical spectrum analyser (OSA) model Bayspec FBGA-F-1525-1565-FP which has wavelength repeatability of up to ±0.1 pm.

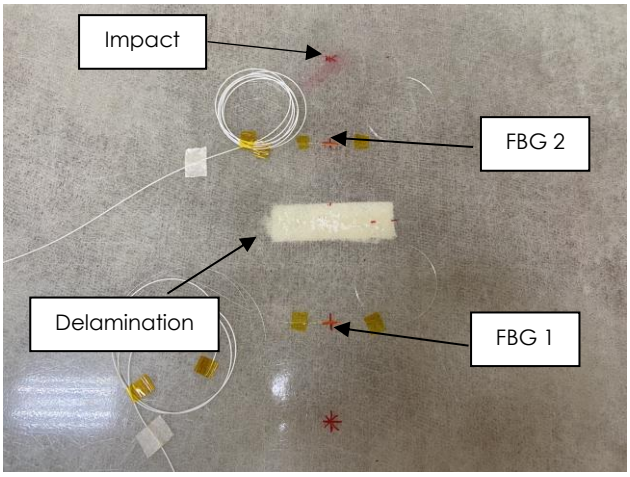

(a)

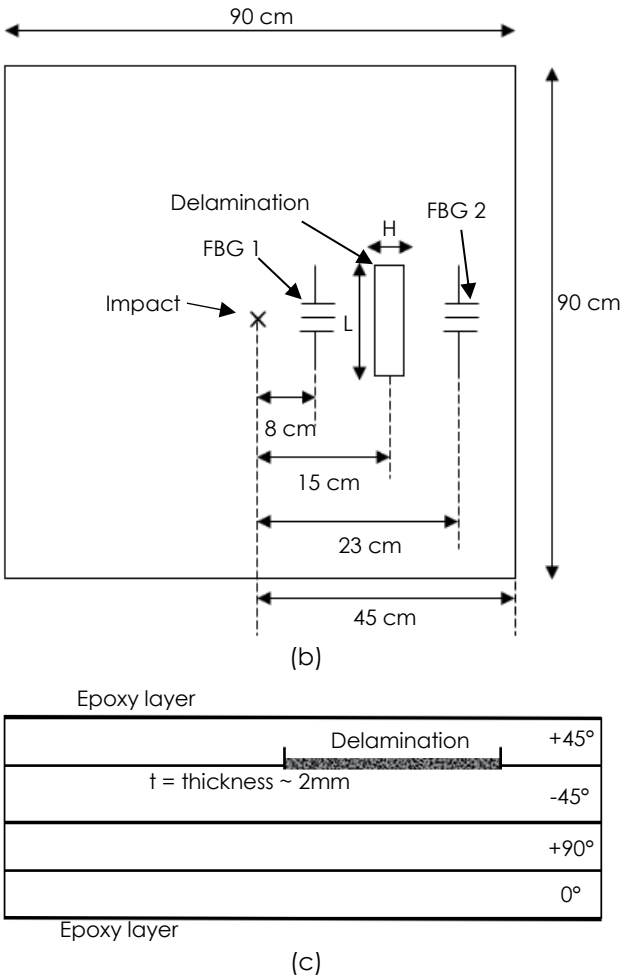

Figure 1 The fabricated specimen: (a) Photo of the composite structure (b) Illustration of the composite structure (c) Arrangement layer of Fiberglass

2.2 Experimental setup

The composite plate was clamped fixed at all four edges, as illustrated in Figure 2. The light signal from the tunable laser source (TLS) was split into two channels via the optical splitter. The first channel was used to illuminate FBG 1 via the optical circulator. Meanwhile, the second channel was used to illuminate FBG 2. The emitted light wavelength from the TLS was set to 1549.72 nm. The TLS used was manufactured by Hangzhou Huatai Optic Tech. Co., Ltd model LTS-2000. The reflected light signals from both FBGs were then channelled to the photodetector (PD). The PD converted the light signals into voltage signals that can be read by the data acquisition (DAQ) device. The PD used was Thorlabs PDA10CS-EC. The DAQ used was NI-9234 by National Instruments with sampling frequency and block size set to 2000 Hz and 2000 samples.

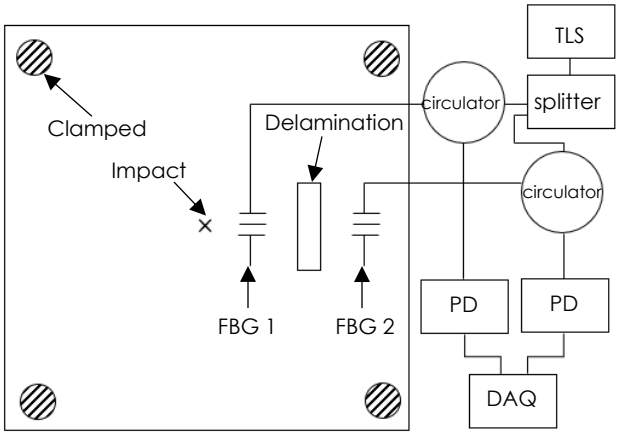

Figure 2 Illustration of the experimental setup

Three impact trials were induced at the centre of the structure. These procedures were first performed on a composite structure with a delamination size of 10 cm × 2 cm. Next, it was repeated on a composite structure with a delamination size of 10 cm × 6 cm. The waveforms captured by FBG 1 and FBG 2 were then analysed for time delay, amplitude and velocity.

3.0 RESULTS AND DISCUSSION

3.1 Time Delay Analysis

Figure 3 (a) and Figure 3 (b) show the time delay in FBG 1 and FBG 2 for delamination sizes of 10 cm × 2 cm and 10 cm × 6 cm. When impact was induced at the centre, acoustic waves started to propagate. FBG 1 was positioned near the impact. Therefore, the waveform will be first captured by FBG 1 followed by FBG 2. Due to this, a time difference between both waveforms was observed.

For a delamination size of10 cm × 2 cm, the peak of the waveform for FBG 1 was recorded at 3.5075 s whereas FBG 2 was recorded at 3.5096 s. Therefore, a time delay of 2.1 ms was obtained for the first trial. For trial 2 and trial 3, a time difference of 2.0 ms and 1.9 ms was obtained. The time difference for all trials showed good consistency with the highest error of 9.52%.

The presence of delamination has also affected the time delay. This can be seen when the delamination size was increased to 10 cm × 6 cm. FBG 1 captured the waveform at 3.3465 s whereas FBG 2 captured the waveform at 3.350 s. This gave a time difference of 3.5 ms for trial 1. For trial 2 and trial 3, a time difference of 3.5 ms and 3.4 ms was obtained. The highest percentage of error between all trials was obtained at 2.86%.

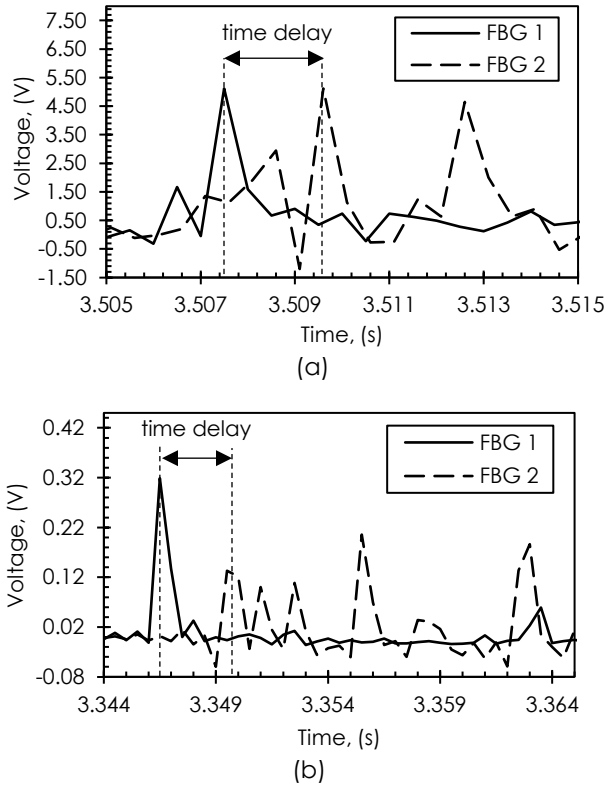

Figure 3 The time delay in FBG 1 and FBG 2 for delamination size of: (a) 10 cm × 2 cm (b) 10 cm × 6 cm

Table 1 shows a summary of the time delay for delamination sizes of 10 cm × 2 cm and 10 cm × 6 cm. An average time delay of 2.0 ms was obtained for a delamination size of 10 cm × 2 cm whereas a 3.47 ms time delay was obtained for a delamination size of 10 cm × 6 cm. The average percentage difference between both delamination sizes was obtained at 42.36%. The high percentage of difference showed that a longer time delay was present in FBG 2. Similar results were also reported by Wang *et al*. [34] and Rekatsinas *et al*. [35]. This could be explained as the waves required to propagate through a larger air gap of delamination before reaching FBG 2.

Table 1 The summary of time delay for delamination size of 10 cm × 2 cm and 10 cm × 6 cm

Delamination size, (*cm*)	Trial	Time delay, (*ms*)
10 × 2	1	2.1
	2	2.0
	3	1.9
	Average	2.0
10 × 6	1	3.5
	2	3.5
	3	3.4
	Average	3.47

3.2 Amplitude Analysis

The waveforms were also analysed for amplitude difference. From Figure 4 (a), the amplitude for FBG 1 was recorded at 5.1216 V whereas the amplitude for FBG 2 was recorded at 5.1162 V. Therefore, the amplitude difference for trial 1 was obtained at 0.0054 V. Trial 2 and trial 3 obtained the amplitude difference of 0.0060 V and 0.0054 V. The highest difference between all the trials was obtained at 10%. For delamination size of 10 cm × 6 cm as in Figure 4 (b), the amplitude difference for trial 1, trial 2 and trial 3 were obtained at 0.1973 V, 0.1973 V and 0.1822 V respectively.

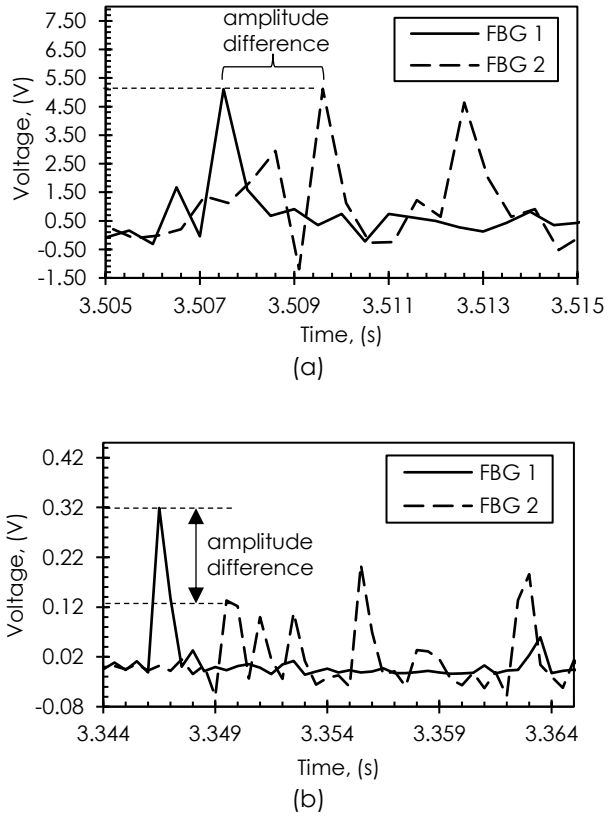

Figure 4 The amplitude difference in FBG 1 and FBG 2 for delamination size of: (a) 10 cm × 2 cm (b) 10 cm × 6 cm

Table 2 shows the summary of amplitude difference for delamination sizes of 10 cm × 2 cm and 10 cm × 6 cm. From the average, it was observed that the amplitude difference for delamination size of 10 cm × 6 cm was much higher as compared to delamination size of 10 cm × 2 cm. The average percentage of the difference between both delamination sizes was obtained at 97.09%. This indicated a much larger amplitude dropped after the delamination as the delamination size increased.

Table 2 The summary of amplitude difference for delamination size of 10 cm × 2 cm and 10 cm × 6 cm

Delamination size, (*cm*)	Trial	Amplitude difference, (*V*)
10 × 2	1	0.0054
	2	0.0060
	3	0.0054
	Average	0.0056
10 × 6	1	0.1973
	2	0.1973
	3	0.1822
	Average	0.1923

Similar results were also reported by Marhenke *et al*. [36] and Hervin *et al*. [17]. This could be explained as the presence of larger delamination resulting in higher attenuation in the wave propagation.

3.3 Velocity Analysis

Velocity analysis was also performed to evaluate the speed of wave which propagated across the delamination area. Figure 5 (a) shows the velocity for the delamination size of 10 cm × 2 cm whereas Figure 5 (b) shows the velocity for the delamination size of 10 cm × 6 cm. The speed of the wave was determined by plotting distance of the sensors from the impact against the time of arrival of the waveform. By determining the response curve of the graph, the velocity for delamination size of 10 cm × 2 cm was obtained at 7.1429 cm/ms. The velocity for trial 2 and trial 3 was obtained at 7.5 cm/ms and 7.8947 cm/ms, as summarised in Table 3.

For a delamination size of 10 cm × 6 cm, the velocity for trial 1, trial 2 and trial 3 were obtained at 4.2857 cm/ms, 4.2857 cm/ms and 4.4118 cm/ms. The average velocity for delamination size of 10 cm × 2 cm was obtained at 7.5125 cm/ms. On the other hand, the average velocity for a delamination size of 10 cm × 6 cm was obtained at 4.3277 cm/ms. From the results, it can be seen that the velocity of the waves reduced with increasing delamination size. The average percentage of the difference between both the delamination size were obtained at 42.39%. According to Murat *et al*. [37], the velocity of the wave depends on the rigidity of the structure. The increased delamination size reduced the rigidity of the structure. Therefore, reduced the velocity of the waves.

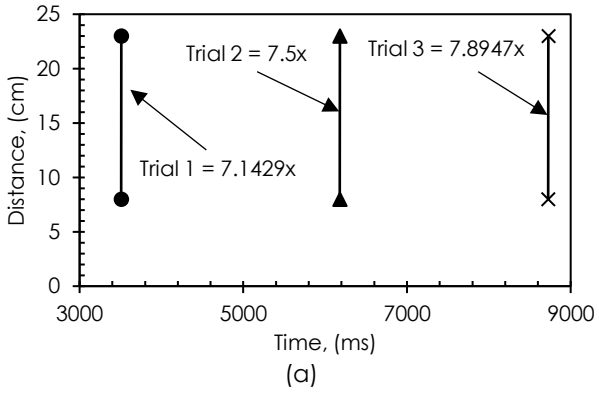

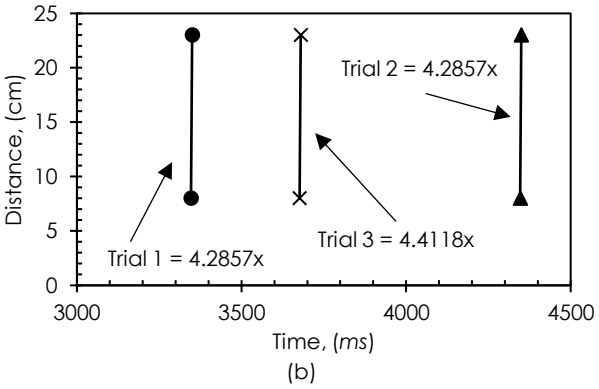

Figure 5 The velocity response curve for delamination size of: (a) 10 cm × 2 cm (b) 10 cm × 6 cm

Table 3 The summary of velocity for delamination size of 10 cm × 2 cm and 10 cm × 6 cm

Delamination size, (*cm*)	Trial	Velocity, (*cm/ms*)
10 × 2	1	7.1429
	2	7.5000
	3	7.8947
	Average	7.5125
10 × 6	1	4.2857
	2	4.2857
	3	4.4118
	Average	4.3277

4.0 CONCLUSION

In this paper, the thin-walled composite structures with delamination sizes of 10 cm × 2 cm and 10 cm × 6 cm were inspected by using an acoustic pitch-catch technique with a pair of FBG sensors. Three different signal parameters were analysed which were the time delay, amplitude difference and velocity difference. Experimental results clearly indicated a significant variation for all parameters with different delamination sizes. In terms of time delay, the average percentage of the difference between both the delamination sizes is 42.36%, while for the amplitude drop the average variation was obtained at 97.09%. For velocity analysis, an average difference of 42.39% was obtained for

both delamination sizes. With these multiple parameters analysis clearly indicating significant changes, the delamination detection via FBG sensors undoubtedly can be an alternative solution for health monitoring of plate-like structures.

Conflicts of Interest

The author(s) declare(s) that there is no conflict of interest regarding the publication of this paper.

Acknowledgement

This research received the financial support from Ministry of Higher Education Malaysia under the Fundamental Research Grant Scheme FRGS/1/2019/TK03/UMP/02/7 @ RDU1901116.

References

[1] Vorathin, E., *et al*. 2018. FBGs Real-time Impact Damage Monitoring System of GFRP Beam based on CC-LSL Algorithm. *International Journal of Structural Stability and Dynamics.* 18(05): 1850075.
[2] Panasiuk, K. and K. Dudzik. 2022. Determining the Stages of Deformation and Destruction of Composite Materials in a Static Tensile Test by Acoustic Emission. *Materials.* 15(1): 313.
[3] Zhang, Y. *et al*. 2021. Cluster Analysis of Acoustic Emission Signals and Infrared Thermography for Defect Evolution Analysis of Glass/Epoxy Composites. *Infrared Physics & Technology*. 112: 103581.
[4] Xu, W. *et al*. 2020. Singular Energy Component for Identification of Initial Delamination in CFRP Laminates through Piezoelectric Actuation and Non-contact Measurement. *Smart Materials and Structures.* 29(4): 045001.
[5] Cuadrado, M. *et al*. 2022. Detection of Barely Visible Multi-impact Damage on Carbon/Epoxy Composite Plates Using Frequency Response Function Correlation Analysis. *Measurement*. 111194.
[6] Derusova, D. *et al*. 2022. Characterising Hidden Defects in GFRP/CFRP Composites by using Laser Vibrometry and Active IR Thermography. *Nondestructive Testing and Evaluation.* 1-19.
[7] Dey, N. *et al*. 2019. Acoustic Wave Technology. Acoustic Sensors For Biomedical Applications. Springer. 21-31.
[8] Alleyne, D. N. and P. Cawley. 1992. The Interaction of Lamb Waves with Defects. *IEEE Transactions on Ultrasonics, Ferroelectrics, and Frequency Control.* 39(3): 381-397.
[9] Takeda, S., Y. Okabe, and N. Takeda. 2002. Delamination Detection in CFRP Laminates with Embedded Small-diameter Fiber Bragg Grating Sensors. *Composites Part A: Applied Science and Manufacturing*. 33(7): 971-980.
[10] Austin, T. S. *et al*. 1999. Damage Assessment in Hybrid Laminates using an Array of Embedded Fiber Optic Sensors. Smart Structures and Materials 1999: Smart Systems for Bridges, Structures, and Highways. SPIE.
[11] Leng, J. and A. Asundi. 2002. Non-destructive Evaluation of Smart Materials by using Extrinsic Fabry–Perot Interferometric and Fiber Bragg Grating Sensors. *Ndt & E International.* 35(4): 273-276.
[12] Takeda, N. *et al*. 2002. Application of Chirped Fiber Bragg Grating Sensors for Damage Identification in Composites. in Smart Structures and Materials 2002: Smart Sensor Technology and Measurement Systems. SPIE.
[13] Takeda, S. *et al*. 2005. Delamination Monitoring Of Laminated Composites Subjected to Low-velocity Impact using Small-diameter FBG Sensors. *Composites Part A: Applied Science and Manufacturing.* 36(7): 903-908.
[14] Ling, H.-y., *et al*. 2005. Utilization of Embedded Optical Fiber Sensors for Delamination Characterization in Composite Laminates using a Static Strain Method. *Smart Materials and Structures.* 14(6): 1377.
[15] Wang, J. and Y. Shen. 2018. Numerical Investigation of Ultrasonic Guided Wave Dynamics in Piezoelectric Composite Plates for Establishing Structural Self-sensing. *Journal of Shanghai Jiaotong University (Science)*. 23(1): 175-181.
[16] Zhao, G. *et al*. 2019. Detection and Monitoring of Delamination in Composite Laminates using Ultrasonic Guided Wave. *Composite Structures.* 225: 111161.
[17] Hervin, F., L. Maio, and P. Fromme. 2021. Guided Wave Scattering at a Delamination in a Quasi-Isotropic Composite Laminate: Experiment and Simulation. *Composite Structures.* 275: 114406.
[18] Aggelis, D. *et al*. 2019. Acoustic Emission Characterization of Damage Sources of Lightweight Hybrid Concrete Beams. *Engineering Fracture Mechanics*. 210: 181-188.
[19] Li, W. *et al*. 2022. Study on Delamination Damage of CFRP Laminates Based on Acoustic Emission and Micro Visualization. *Materials.* 15(4): 1483.
[20] Saeedifar, M. *et al*. 2018. Barely Visible Impact Damage Assessment in Laminated Composites using Acoustic Emission. *Composites Part B: Engineering.* 152: 180-192.
[21] Ismail, N. *et al*. 2019. Fiber Bragg Grating-based Fabry-Perot Interferometer Sensor for Damage Detection on Thin Aluminum Plate. *IEEE Sensors Journal*. 20(7): 3564-3571.
[22] Teixeira, J. G. V., *et al*. 2014. Advanced Fiber-optic Acoustic Sensors. *Photonic Sensors*. 4(3): 198-208.
[23] Ameen, O. F. *et al*. 2016. Comparison of Water Level Measurement Performance for Two Different Types of Diaphragm using Fiber Bragg Grating based Optical Sensors. *Jurnal Teknologi.* 78(6-11): 97-101.
[24] Harun, S. W., P. Poopalan, and H. Ahmad. 2002. Fabrication of Fiber Bragg Gratings in High Germania Boron Co-Doped Optical Fiber by the Phase Mask Method. *Jurnal Teknologi.* 11-18.
[25] Salih, Y. M., Y. Munajat, and H. Bakhtiar. 2016. Response of FBG-bonded Plastic Plate at Different Locations of Applied Stress. *Jurnal Teknologi.* 78(6-11): 77-83.
[26] Vorathin, E. and Z. Hafizi. 2020. Bandwidth Modulation and Centre Wavelength Shift of a Single FBG for Simultaneous Water Level and Temperature Sensing. *Measurement*. 163: 107955.
[27] Vorathin, E. *et al*. 2019. Temperature-insensitive Pressure Transducer based on Reflected Broadened Spectrum with Enhanced Sensitivity. *Sensors and Actuators A: Physical.* 288: 61-66.
[28] Bucaro, J. *et al*. 2013. Compact Directional Acoustic Sensor using a Multi-Fiber Optical Probe. *The Journal of the Acoustical Society of America.* 133(2): 832-841.
[29] Bucaro, J. A. *et al*. 2005. Miniature, High Performance, Low-Cost Fiber Optic Microphone. *The Journal of the Acoustical Society of America.* 118(3): 1406-1413.
[30] He, G. and F.W. Cuomo. 1991. Displacement Response, Detection Limit, and Dynamic Range of Fiber-Optic Lever Sensors. *Journal of Lightwave Technology*. 9(11): 1618-1625.
[31] Teixeira, J. G., *et al*. 2014. Advanced Fiber-Optic Acoustic Sensors. *Photonic Sensors*. 4(3): 198-208.
[32] Imai, M., T. Ohashi, and Y. Ohtsuka. 1980. Fiber-Optic Michelson Interferometer using an Optical Power Divider. *Optics Letters.* 5(10): 418-420.
[33] Imai, M., T. Ohashi, and Y. Ohtsuka. 1981. High-sensitive All-Fiber Michelson Interferometer by Use of Differential Output Configuration. *Optics Communications*. 39(1-2): 7-10.
[34] Wang, F. *et al*. 2022. Quantitative Non-destructive Evaluation of CFRP Delamination Defect using Laser Induced Chirp-pulsed Radar Photothermal Tomography. *Optics and Lasers in Engineering.* 149: 106830.

[35] Rekatsinas, C., N. Chrysochoidis, and D. Saravanos. 2021. Investigation of Critical Delamination Characteristics in Composite Plates Combining Cubic Spline Piezo-layerwise Mechanics and Time Domain Spectral Finite Elements. *Wave Motion*. 106: 102752.
[36] Marhenke, T. *et al*. 2018. Modeling of Delamination Detection Utilizing Air-coupled Ultrasound in Wood-based Composites. *NDT & E International*. 99: 1-12.
[37] Murat, B. I., P. Khalili, and P. Fromme. 2016. Scattering of Guided Waves at Delaminations in Composite Plates. *The Journal of the Acoustical Society of America*. 139(6): 3044-3052.